FORSCHUNGSZENTRUM ROSSENDORF FZR

WISSENSCHAFTLICH-TECHNISCHE BERICHTE
FZR-257
April 1999
ISSN 1437-322X

Hans-Georg Willschütz

CFD-Calculations to a Core Catcher Benchmark

Herausgeber:
FORSCHUNGSZENTRUM ROSSENDORF
Postfach 51 01 19
D-01314 Dresden
Telefon (03 51) 26 00
Telefax (03 51) 2 69 04 61

Als Manuskript gedruckt

FORSCHUNGSZENTRUM ROSSENDORF

WISSENSCHAFTLICH-TECHNISCHE BERICHTE

FZR-257

April 1999

Hans-Georg Willschütz

CFD-Calculations to a Core Catcher Benchmark

Abstract

There are numerous experiments for the exploration of the corium spreading behaviour, but comparable data have not been available up to now in the field of the long term behaviour of a corium expanded in a core catcher. The difficulty consists in the experimental simulation of the decay heat that can be neglected for the short-run course of events like relocation and spreading, which must, however, be considered during investigation of the long time behaviour.
Therefore the German GRS, defined together with Battelle Ingenieurtechnik a benchmark problem in order to determine particular problems and differences of CFD codes simulating an expanded corium and from this, requirements for a reasonable measurement of experiments, that will be performed later.
First the finite-volume-codes Comet 1.023, CFX 4.2 and CFX-TASCflow were used. To be able to make comparisons to a finite-element-code, now calculations are performed at the Institute of Safety Research at the Forschungszentrum Rossendorf with the code ANSYS/FLOTRAN.
For the benchmark calculations of stage 1 a pure and liquid melt with internal heat sources was assumed uniformly distributed over the area of the planned core catcher of a EPR plant.
Using the Standard-k-ε-turbulence model and assuming an initial state of a motionless superheated melt several large convection rolls will establish within the melt pool. The temperatures at the surface do not sink to a solidification level due to the enhanced convection heat transfer. The temperature gradients at the surface are relatively flat while there are steep gradients at the ground where the no slip condition is applied. But even at the ground no solidification temperatures are observed.
Although the problem in the ANSYS-calculations is handled two-dimensional and not three-dimensional like in the finite-volume-codes, there are no fundamental deviations to the results of the other codes.

Content

1. **Introduction** 1

2. **Physical problem and numerical approach** 2

3. **Description of the model** 4
   - **3.1 Material Properties** 4
     - **3.1.1 Dynamic viscosity and thermal conductivity** 4
     - **3.1.2 Density and heat capacity** 4
   - **3.2 The element *fluid141*** 5
   - **3.3 Geometry and Meshing** 6
   - **3.4 Initial and boundary conditions** 7
     - **3.4.1 Thermodynamic initial and boundary conditions** 7
     - **3.4.2 Fluiddynamic initial and boundary conditions** 7
   - **3.5 Solution options** 8

4. **Results of the 2D calculations** 9
   - **4.1 Time dependent behaviour of the melt** 9
   - **4.2 The temperature field after 2100 s** 12
   - 4.3 Comparison with the FVM-codes 13

5. **Conclusion and Outlook** 14

6. **References** 15

1. Introduction

For future nuclear power plants it is demanded that there are no consequences for the environment and the population even in the closest vicinity of the plant during and after every possible accident scenario [1].
This includes the hypothetical scenario of a severe accident with subsequent core meltdown, formation of a melt pool in the reactor pressure vessel (RPV) lower head, failure of the vessel and relocation into the reactor pit and/or the core catcher. At present different core catcher concepts which are used for the control, stabilization and cooling of the melt are examined.
While there are numerous experiments for the exploration of the spreading behaviour of corium [2; 3], comparable data have not yet been available in the field of the long term behaviour of a corium expanded in the core catcher up to now. The difficulty consists in the experimental simulation of the decay heat that can be neglected for the short-run course of events like relocation and spreading, which must, however, be considered during investigation of the long time behaviour.
The German GRS defined together with Battelle Ingenieurtechnik a benchmark problem, in order to determine particular problems and differences of computational fluid dynamics codes (CFD codes) during simulation of ex-vessel-corium. In this case, the codes CFX-TASCflow, CFX 4.2 and Comet 1.023 working with finite-volume-method (FVM) were first used. To be able to make comparisons to a code based on finite-element-method (FEM), later also ANSYS/FLOTRAN calculations were carried out at the Institute of Safety Research at the Forschungszentrum Rossendorf.
For the calculations a pure and liquid melt with a homogenous internal heat source was assumed. The melt was distributed uniformly over the spreading area of the European Pressurized Water Ractor (EPR) core catcher concept [4, 5].
While the FVM-code calculations were performed with three dimensional models using a simple symmetry, the problem was modeled two-dimensional with ANSYS due to limited CPU performance. In addition, the 2D results of ANSYS should allow a comparability at the planned second stage of the calculations. In this second stage, the behaviour of a segregated metal oxide melt should be examined. However, first estimates and pre-calculations showed that a 3D simulation of the problem for no code is reasonable with at this time available computer performance, consequently, the availability of two-dimensional ANSYS results for both stages of the benchmark calculations is useful for the purpose of comparison.
In chapter 2 a short introduction to the considered physical problem and the numerical approach is given. The construction of the FE-model, the definition of the boundary conditions and property values are explained in chapter 3. The results are then represented and discussed in chapter 4. Chapter 5 finishes with the conclusion and outlook.

2. Physical problem and numerical approach

For an assessment of the physical problem considered in this benchmark it is useful to calculate and discuss the main dimensionless parameters resulting from geometry, boundary conditions and material properties.
For the CFD-Code calculations a homogeneous melt with internal heat sources has been chosen. Although artificial melt properties have been assumed, its viscosity is similar to a liquid metal corium whereas the heat conductivity is comparable to a oxidic corium. The EPR core catcher concept was the geometrical basis.
The assumed geometrical figures, boundary conditions and material properties are:

$H=0.3$ m	: vertical Height of the completely spreaded melt,
$q_V=500$ kW/m^3	: internal volumetric heat generation rate,
$q_W=20$ kW/m^2	: heat flux through vertical walls,
$q_B=25$ kW/m^2	: heat flux to the ground,
$q_O=125$ kW/m^2	: heat flux to the free surface (has to be adjusted for equilibrium),
$\rho_0=6510$ kg	: reference density at $T_0=2275$ K,
$\eta=2.5$ mPa s	: dynamic viscosity,
$\nu=3.84\ 10^{-7}$ m^2/s	: kinematic viscosity,
$\lambda=2.2$ W/m K	: heat conductivity,
$c_{p,0}=610$ J/kg K	: heat capacity at $T_0=2275$ K,
$a=5.57\ 10^{-7}$ m^2/s	: thermal diffusivity,
$\beta=5.0\ 10^{-5}$ 1/K	: volumetric heat expansion coefficient and
$g=9.81$ m/s^2	: gravitational acceleration.

The dimensionless parameter denoting the relationship between the temperature and the flow field boundary layers is called Prandtl-number, which can be calculated for the considered problem to:

$$Pr = \frac{\nu}{a} = 0.69$$

A Prandtl-number smaller than 1 means that the boundary layer of the flow field is thinner than the bundary layer of the temperature field. For the discussed problem the Prandtl-number is slightly smaller than 1, that means the two fields are in general comparable.

The internal Rayleigh-number (Ra) is the main characteristic dimensionless parameter describing the considered problem. It is the product of the Grashoff (Gr), Prandtl (Pr) and Dammköhler (Da) numbers [6, 7]. With the above listed properties the internal Rayleigh-number is calculated to:

$$Ra_i = Gr\ Pr\ Da = \frac{g\beta q_V H^5}{\nu a \lambda} = 1.26\ 10^{12}$$

It can be stated that convection flow due to internal heat sources is always turbulent, because the range of a laminar flow regime is very small. For example: The critical Rayleigh-number for a horizontal fluid layer heated from below (Ra=Gr Pr) is 10^4 at a comparable Prandtl-number [8].

Theoretically there are two possibilities for the numerical treatment of this convection problem: the first one could be the direct numerical simulation (DNS) the second one is the use of a turbulence model. The principle of DNS requires a numerical grid or mesh that is densely enough to solve each vortex in the flow field correctly in space and time. All equations of conservation can be solved without any further assumptions or models. But despite the fast growing computational power it is impossible to solve a convection flow with internal heat sources for such large geometries and time ranges within the near future.

That is why a turbulence model has to be applied. All codes used the so called Standard-k-ε-model [9]. This is a two-equation-model where the effective turbulent viscosity and thermal conductivity are calculated by means of the turbulent kinetic energy and the energy dissipation rate.

Close to walls the "Log Law of the Wall" is applied. This law calculates a near wall viscosity in consistence to experimental found velocity profiles by means of the dimensionless wall distance Y^+. The value of Y^+ depends on the size of the wall elements. It is recommended to control the Y^+-value to check the accuracy of the model.

3. Description of the model

For the modeling of a fluiddynamic problem with the FE program ANSYS the module FLOTRAN is required. The procedure for the fluiddynamic modeling is similar to the procedure in the case of mechanical or thermodynamic FE problems in solids. The material properties (see 3.1) are first determined in the preprocessor, the element type (see 3.2) is then selected. After this the geometry of the model is defined (see 3.3) and the model is meshed.
The last step during preprocessing is the determination of the initial and boundary conditions for the corresponding nodes of the model (see 3.4).
After this the options for the solution of the problem are determined in the solution processor (see 3.5). The calculation with the *solve* command is finally started.
The space- or time-controlled representation of the results can then be carried out in the two corresponding postprocessors.
All quantities in the model are SI units (m, kg, s); Temperatures are indicated in K.

3.1 Material Properties

The material properties are determined within the macro **fdatsatz.mac**. The properties can be independent on temperature, can be calculated according to a temperature dependent function or can depend on the temperature and be interpolated between the values of a table defined by the user.
With the command *FLDATA7,PROT,xxxx,yyyy* the appropriate property model is activated. From this choice further commands are required in order to model the desired material properties.

3.1.1 Dynamic viscosity and thermal conductivity

At the considered temperature range, the dynamic viscosity is assumed to be constant at μ=2.5 10^{-3} Pa s. The thermal conductivity is also defined as constant with λ=2.2 W/mK.
The equivalent commands within the ANSYS/FLOTRAN routine are:

FLDATA7,PROT,visc,const	:	constant viscosity,
FLDATA8,NOMI,visc,2.5e-3	:	nominal value of viscosity,
FLDATA7,PROT,cond,const	:	constant thermal conductivity,
FLDATA8,NOMI,cond,2.2	:	nominal value of the thermal conductivity.

So these two material properties for the thermofluid dynamic calculations are determined.

3.1.2 Density and heat capacity

For temperature dependent density, the Boussinesq-approximation can not be selected at ANSYS in the actual sense as it is possible in the case of the FVM codes. With the usual Boussinesq-approximation the density becomes constant in all equations except

for the buoyancy term of the equation of motion. Contrary to this, the temperature tracking of density is considered completely in all equations in the ANSYS-model.
In the FE-Modell, two temperatures are defined for a linear interpolation:
$\rho(T=1600\ K)=6730\ kg/m^3$ and
$\rho(T=2400\ K)=6469\ kg/m^3$.
These values correspond to a volumetric coefficient of expansion of $\beta=10^{-5}$ 1/K, at a reference density of $\rho_0(T_0=2275\ K)=6510\ kg/m^3$, as it was determined for the benchmark calculations.
The specific heat capacity is defined according to the same procedure:
$c_p(T=1600\ K)=590$ J/kgK and
$c_p(T=2400\ K)=618$ J/kgK.
Besides these two quantities must be declared as temperature dependent so that they are updated after every global iteration.
The corresponding commands are:

MPTEMP,1,1600,2400	: temperature points,
MPDATA,dens,1,1,6730,6469	: corresponding density,
MPDATA,spht,1,1,590,618	: corresponding heat capacity,
FLDATA7,PROT,dens,table	: density is to be interpolated according to the table,
FLDATA7,PROT,spht,table	: heat capacity is to be interpolated according to the table,
FLDATA13,VARY,dens,true	: variable density, i. e. update after every global iteration,
FLDATA13,VARY,spht,true	: variable heat capacity.

With *MPTEMP* the temperature base points are determined and the corresponding property values on these points are assigned with *MPDATA*.

3.2 The element *fluid141*

The program ANSYS/FLOTRAN makes two elements available for CFD calculations: *fluid141* for 2D problems and *fluid142* for 3D applications. The 2D element *fluid141* employed in the case of the calculations is discussed here. It has four nodes, one in each corner as a rectangular (quadrilateral) element.
Triangular elements with three nodes are also possible, however, it is reasonable for meshing, to use a mapped meshing with square elements since a better convergence and more precise results are generally achieved in particular if a turbulence model is used.
Depending on problem to be calculated, every node has between 1 and 12 degrees of freedom (DOF). The minimum number of DOF results for a thermodynamic problem where only the temperature field is solved.
If a 2D-fluiddynamic problem is considered without solution of the temperature field, 3 degrees of freedom are to be solved (v_x, v_y, p) for the laminar case and 5 for the turbulent case due to the activation of the k-epsilon-turbulence model. If a temperature field must be solved additionally, the temperature degree of freedom (T) is added.
The maximal number of 12 DOFs results with multi-component mixing problems. ANSYS/FLOTRAN allows a maximum of 6 different species, with their mass fractions adding up to 1. Therefore, 5 further DOFs which correspond to the concentrations of the

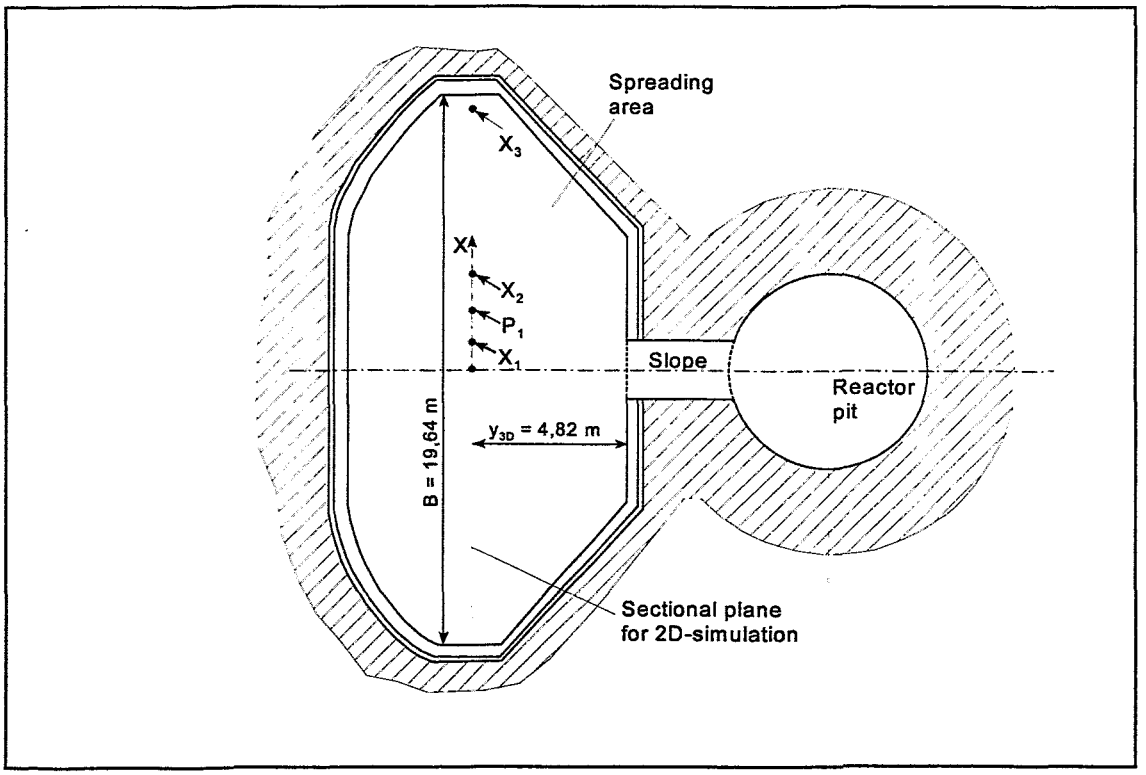

Fig. 1: Top view of the EPR core catcher configuration.

components are added (Y_1-Y_5).
With one component considered in this report, it follows that 6 degrees of freedom (v_x, v_y, p, k, epsilon, T) are to be calculated.

3.3 Geometry and Meshing

As mentioned in the introduction 2D simulations of the problem are performed with ANSYS. The considered vertical plane represents a cut through the core catcher on the position y_{3D}=4.82 m (s. Fig. 1). The height of the melt layer is H=0.3 m, the width is B=9.64 m if symmetry is used and B=19.28 m in the case of modeling the full width of the core catcher. The ANSYS-model denotes the upright axis as y-axis and the horizontal direction as x-axis (s. Fig. 2). At the following, all co-ordinate information refers to the ANSYS definition.
In vertical direction there are 14 elements, what in case of the selected element type fluid141 corresponds to 15 nodes in an equidistant vertical configuration. A division of 80 equidistant elements on a length of 9.60 m was chosen for the horizontal direction. At the upright wall, a column with narrower elements (width b=0.04 m) was used for a better modeling of the boundary conditions, so that in the half symmetrical case there are arranged 81 elements in total in horizontal direction and/or 162 in the case of modeling of the entire 2D problem.
For the half symmetrical 2D model there are 1134 elements of the type fluid141 with 1230 nodes in total.

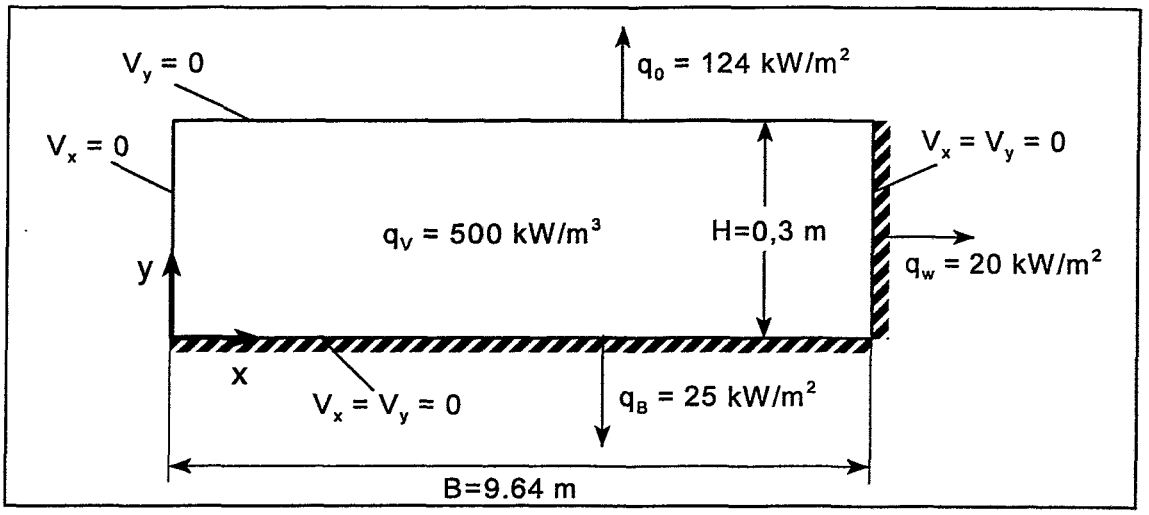

Fig. 2: Thermo- and fluiddynamic boundary conditions of the 2D-simulation.

3.4 Initial and boundary conditions

For the benchmark calculations, the thermodynamic initial and boundary conditions were essentially prescribed. Additional fluiddynamical limiting conditions result from the problem to be modelled.

3.4.1 Thermodynamic initial and boundary conditions

At the beginning the melt has a uniform temperature of T_0=2275 K (command: *ic,all,temp,2275*). The inner heat sources were modeledaccording to the benchmark requirements with q_v=500 kW/m^3 (*bf,all,hgen,5.0e5*). These two conditions refer to all nodes of the model (*nsel,all*).
The heat flux into the sidewalls is q_w=20 kW/m^2, that into the ground q_B=25 kW/m^2. For modeling these boundary conditions, the nodes on the corresponding positions were selected (e.g. *nsel,s,loc,y,0*) and applied with the heat flow to be modeled(e.g. *sf,all,hflux,-2.5e4*). The heat flow on the surface should be chosen in such a way, that the total heat balance is in equilibrium. In this way, for the 2D model resulted a heat flow of q_0=123.146 kW/m^2 which was modeledanalogously to the other surface loads.

3.4.2 Fluiddynamic initial and boundary conditions

At the starting time t=0 s the melt is not in motion what corresponds to default setting of ANSYS. For modeling the volume force of gravity, an acceleration is prescribed in upright direction (*acel,,9.81*). For all nodes that are at a wall, the wall boundary condition is prescribed with the no slip condition (*d,all,vx,0; d,all,vy,0*). On the other hand, the free slip condition applies to the nodes at the free surface and on the symmetry line i.e., the component of velocity is only set to zero normally to the boundary surface.

3.5 Solution options

Because the program ANSYS/FLOTRAN can be applied to many physical problems, there are different options for the solution of the FE-model. These options must be activated or deactivated according to the considered problem. The investigated melt pool scenario requires the solution of a transient and turbulent temperature and flow field of a single phase fluid consisting of one species. The commands to be executed for the consideration of the specific problem and model features are also contained in the macro **fdatsatz.mac.**
The most important commands that differ from the ANSYS-default setting are:

FLDATA1,SOLU,TURB,true	: activates the k-ε-turbulence modell,
FLDATA1,SOLU,TEMP,true	: activates the solution of the temperature field,
FLDATA1,SOLU,TRAN,true	: activates a transient solution,
FLDATA4,TIME,STEP,1.0	: time step size (dt=1.0 s),
FLDATA4,TIME,TEND,2100	: specifies the transient end time of the solution,
FLDATA5,OUTP,YPLU,true	: activates saving of the y^+-values,
FLDATA18,METH,PRES,1	: activates TDMA (Tri-Diagonal Matrix Algorithm) for the solution of the pressure field,
FLDATA18,METH,TEMP,3	: activates PCRA (Preconditioned Conjugate Residual Algorithm) for the solution of the temperature field.

The default value of 20 for the maximum number of global iterations per time step has not been modified. After every global iteration the temperature-dependent properties are updated. The time step size and the transient end time of the solution have been defined for the benchmark to dt=1.0 s and t_{end}=2100 s respectively. These time step conditions were postulated for all participating codes for comparability.

4. Results of the 2D calculations

In the following the essential parameters, courses of events and results of the transient 2D simulation of the one component-melt are explained and discussed.

4.1 Time dependent behaviour of the melt

At the beginning of the calculation the melt has a uniform temperature of T_0=2275 K and is motionless. After this the temperatures in the boundary layers to the ground, to the sidewall and the free surface sink on account of the small thermal conductivity of the oxidic melt (λ=2.2 W/mK). The temperature drop is proportional to the amount of the heat flow, therefore, the temperature minima are at the upper surface of the melt pool. On the other hand the temperatures in the interior of the pool increase. In the diagram Fig. 3, the temperature is represented for node 442 (point P1 in Fig. 1) with the co-ordinates x=2.4 m and y=0.15 m which is in the vertical center of the pool, the initial linear temperature rise in the interior of the melt configuration can be seen clearly.
After some 80 s, the melt stratification becomes unstable at the surface on account of the increase of density of colder melt. Irregularly distributed plumes are found.
The node represented in Fig. 3 is near such a plume, that explains the strong temperature drop after 85 s of almost 25 K within 15 s.
For illustration the temperature field after 85 s is shown in Fig. 4.
While the melt in the center of a plume moves down, surrounding fluid flows upwards for volume compensation. This course of events can be pursued in the diagram Fig. 5, the upright component of velocity v_y of node 442 is represented over time. Since the node is next to the low temperature plume, the upright component of velocity achieves a maximum at 90 s.
The minimum for the horizontal component v_x can be explained analogously, the

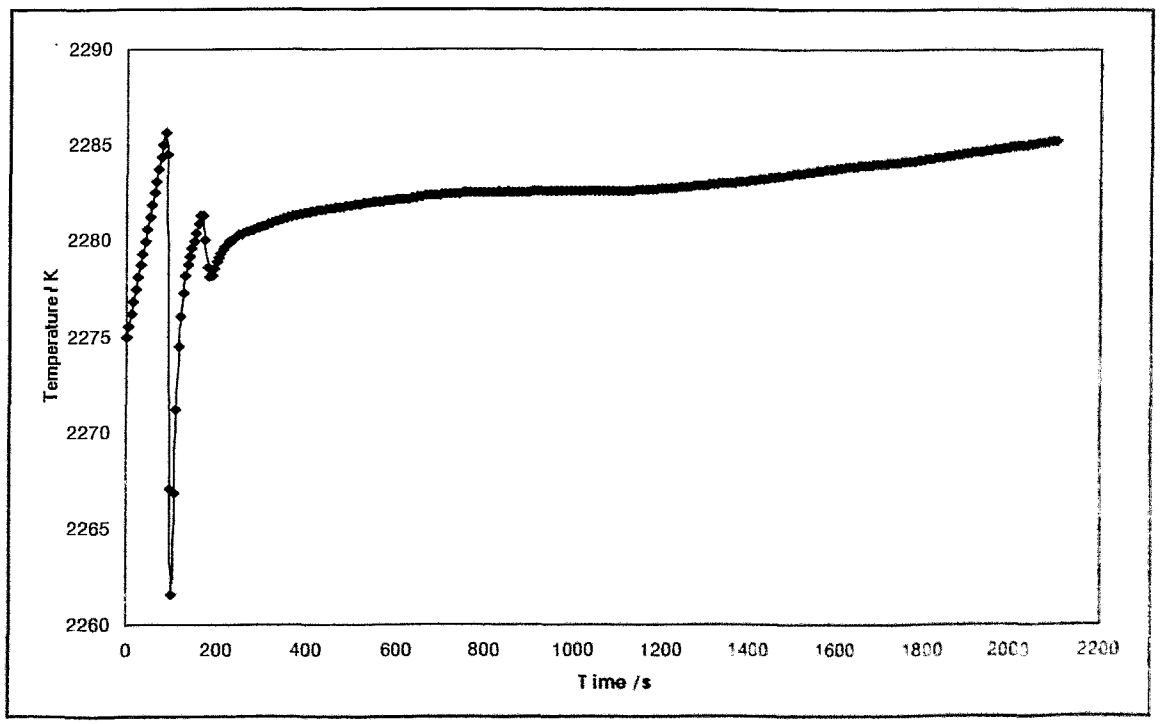

Fig. 3: Temperature vs. time at point P_1(x=2.4 m; y=0.15 m).

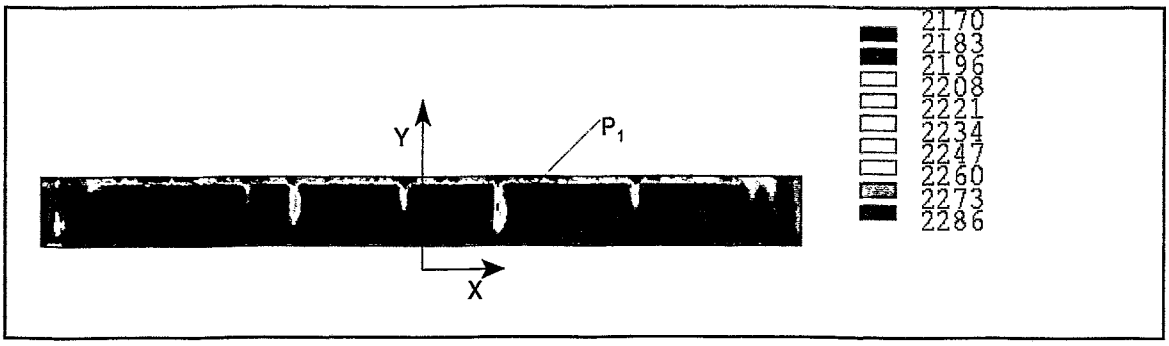

Fig. 4: Temperature field for whole section after 85 s.

velocity is represented in Fig. 6: Node 442 is to the right from the plume. While the plume shifts itself down, the surrounding fluid moves towards the plume, which means that the fluid located to the right is sped up into the minus x-axis direction.
After the plume has achieved the ground of the pool, it tears off since the density and/or temperature differences are first relocated from the melt pool upper surface. This strictly speaking only applies to the temperature field because the plume initialized a velocity field which develops a Rayleigh-Bénard-convection through the mutual influencing of neighboring plumes.
Between two plumes two screwing convection rolls are established. (This simple description applies to the two-dimensional case, in the 3D-case a hexagonal cell structure develops.)
The initial roll number and structure after some 120 s appears chaotic. Through coalescence of side-by-side rolls, the number decreases and a regular structure develops itself. Two kinds of coalescence are to be distinguished:
rolls lasting side-by-side with equidirectional rotation have aim to merge, while rolls with opposite rotational sense can disturb each other and the bigger and/or faster rotating one can remove the smaller/slower one.
This course of events essentially is finished after 300 s, at this time 18 rolls with

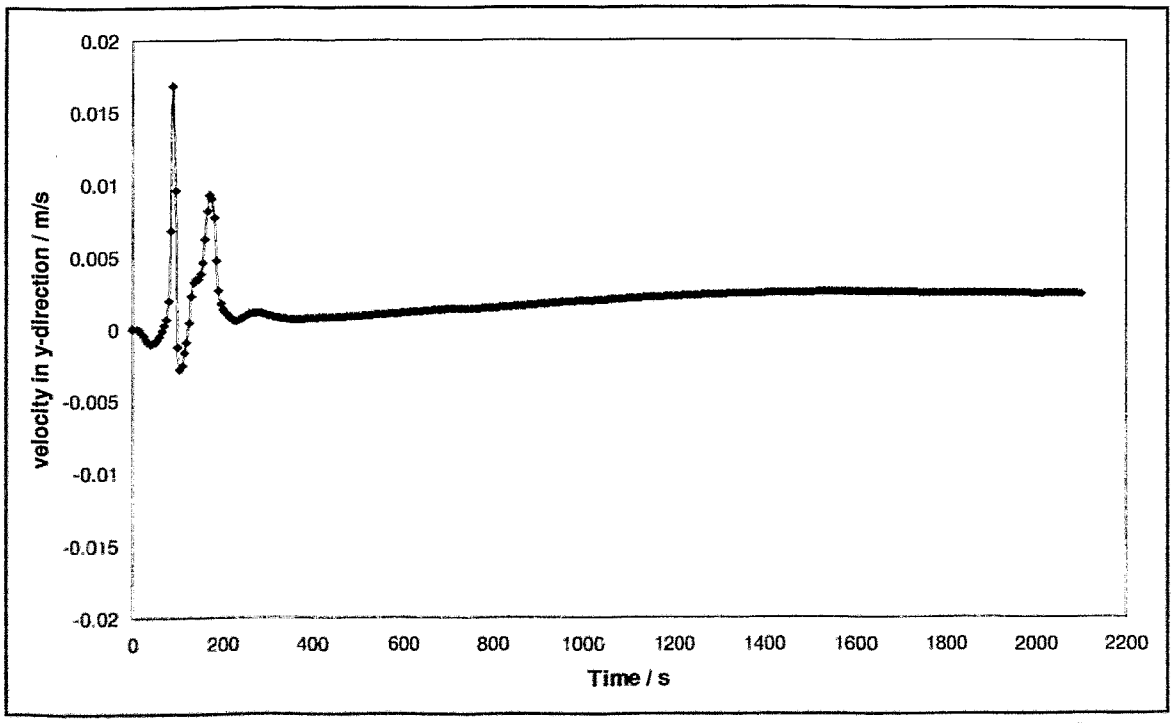

Fig. 5: Vertical velocity component vs. time at point P_1(x=2.4 m; y=0.15 m).

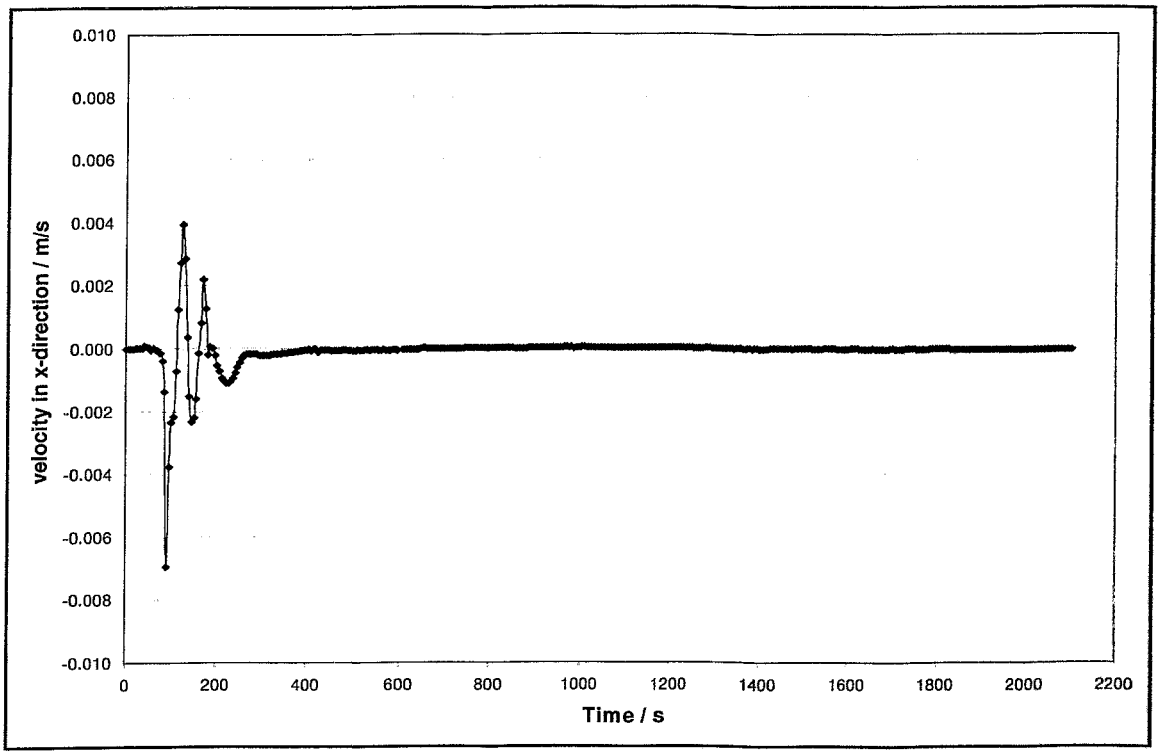

Fig. 6: Horizontal velocity component vs. time at point P_1(x=2.4 m; y=0.15 m).

alternating rotational sense can be observed over the entire width of the EPR core catcher of 19.64 m, i.e., the average width of a roll is 1 m (s. Fig. 7).
In the time dependent diagrams it can be recognized that the velocity and temperature field are in a quasi-stationary state after 300 s.
After this time, two new rolls form themselves slowly at the two outer sides of the melt configuration. They are driven besides by the heat losses at the sidewalls, as a result, they receive a greater spin than the other rolls. The two exterior rolls increase slowly to the middle of the corium pool. Each of them removed the two rolls formerly located at

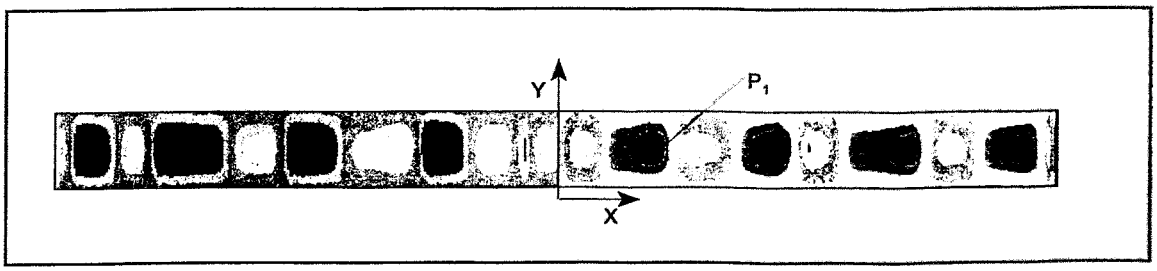

Fig. 7: Streamlines for whole section after 300 s (leftturn - positive - red; rightturn - negative - blue).

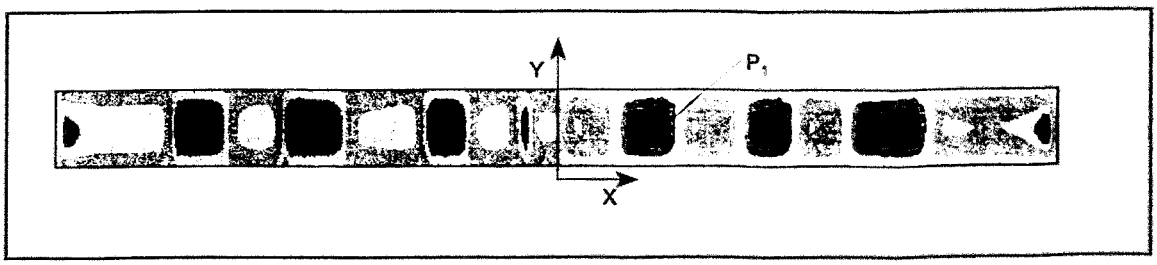

Fig. 8: Streamlines for whole section after 2100 s (leftturn - positive - red; rightturn - negative - blue).

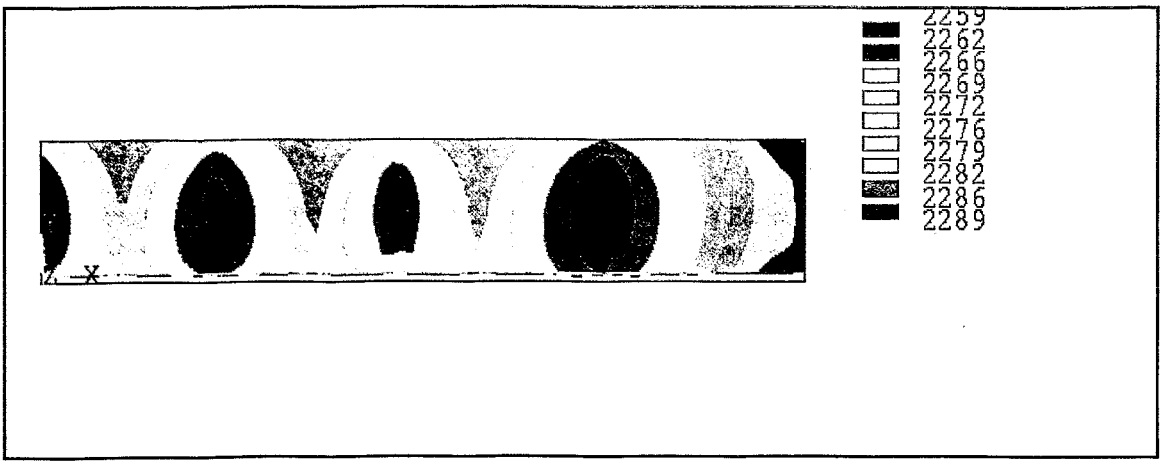

Fig. 9: Temperature field for half section after 2100 s. (Temperatures below 2259 K are grey).

the walls until the end of the calculation after 2100 s, so that 16 rolls can be observed then (s. Fig. 8). This evolution seems not to be finished at the end of the considered calculation time period, on the other hand, it is probable that the large rolls near the vertical walls are not stable in the three dimensional case.

4.2 The temperature field after 2100 s

For the benchmark calculation, temperature and velocity field should be recorded according to the end time of 2100 s. In particular the number of the rolls in the plane with y_{3D}=4.82 m is of interest; it was discussed in the section 3.1.
The temperature field after 2100 s is represented in Fig. 9. It was determined that the temperature scale extends over 30 K - starting from the maximum temperature downwards. The maximum temperature to be found is T_{max}=2289 K, consequently the scale ends at a lower bound of T=2259 K. All temperatures below 2259 K are represented grey.
In Fig. 9, one recognizes 4 zones with higher temperatures, these are the ascending zones of two neighboring convection rolls with counterrotating sense.
The biggest roll is at the right end of the section, it turns to the right (mathematically negative) and extends from the wall to the center of the first high temperature region. On account of the size of the roll and the additional heat losses at the right wall, it shows the greatest temperature difference of all convection rolls between hot buoyancy zone and cold sinking zone.
In Fig. 10 the temperature profile is represented over the height of the melt layer (H=0,3 m) for three X-coordinate positions (cf. Fig. 1). The total temperature level close at the sidewall (X_3=9.5 m) is lower than towards the center of the corium pool (X_2=4,0 m; X_1=1,0 m).
The large temperature gradients on the ground result from the no-slip-condition because a small kinetic turbulent energy is calculated by the turbulence model in the wall region, this leads to a small effective thermal conductivity.
With the chosen CFD-model restrictions and an assumed solidification temperature of 2175 K of the oxidic melt it can be stated that there is no crust formation at the surface due to the high convection heat transfer.

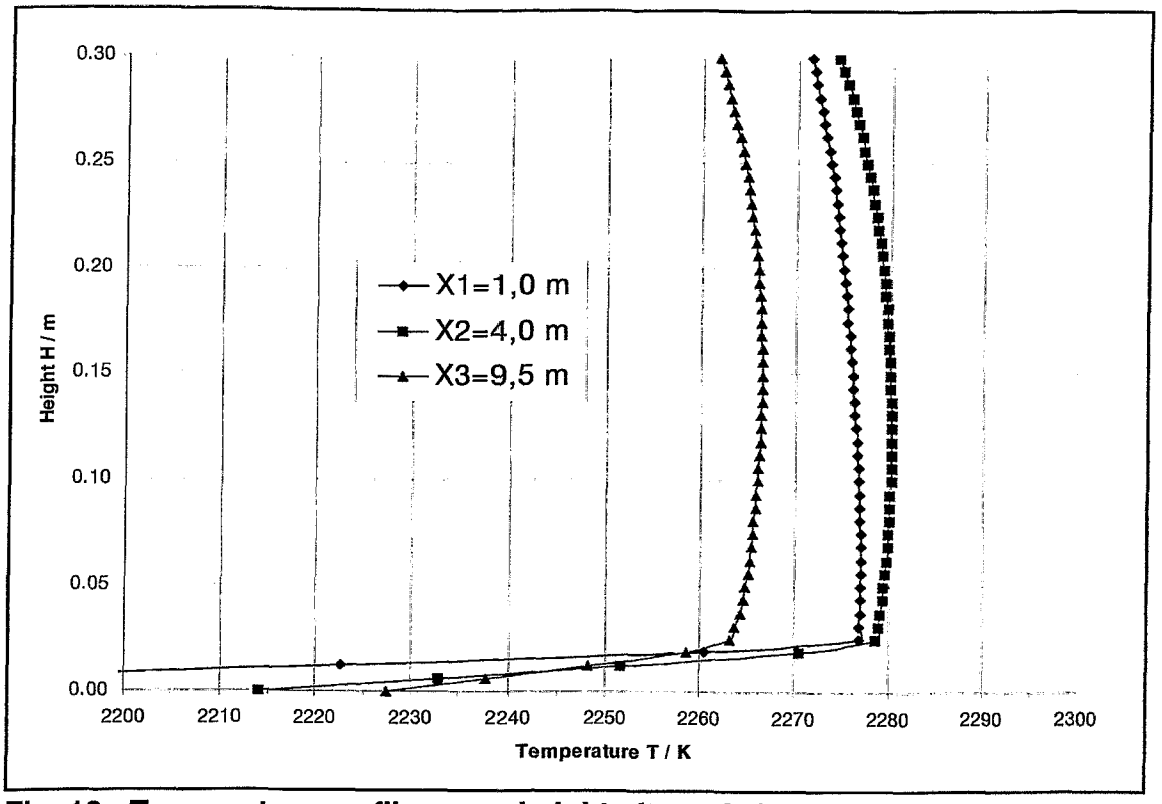

Fig. 10: Temperature profiles over height after t=2100 s.

4.3 Comparison with the FVM-codes

Considering the vertical temperature profiles over height for all codes at position X_3 (s. Fig. 11) it can be stated that the codes CFX 4.2 and Comet 1.023 calculate steeper temperature gradients at the free surface than at the ground. But CFX 4.2 calculates a several times higher temperature difference within the boundary layers. On the other hand CFX-TASC flow calculates generally a steeper gradient at the ground than at the surface. In fact the temperature gradient at the surface is relatively flat.
Looking at the temperature profiles calculated by ANSYS/FLOTRAN the following comparisons can be made:

- The steep gradients on the ground are comparable with that ones calculated by CFX 4.2 and CFX-TASCflow. Although the boundary layer calculated by ANSYS has a greater vertical extension.
- At the free surface the ANSYS temperature curves are comparable with those from CFX-TASCflow.

For the ANSYS results the explanation is: On account of the free slip condition, the turbulence model calculates high effective thermal conductivities, those are up to 3 magnitudes above the laminar conductivity, that is the reason for the small temperature gradients despite of the five times higher heat flow to the surface compared to that to the ground.

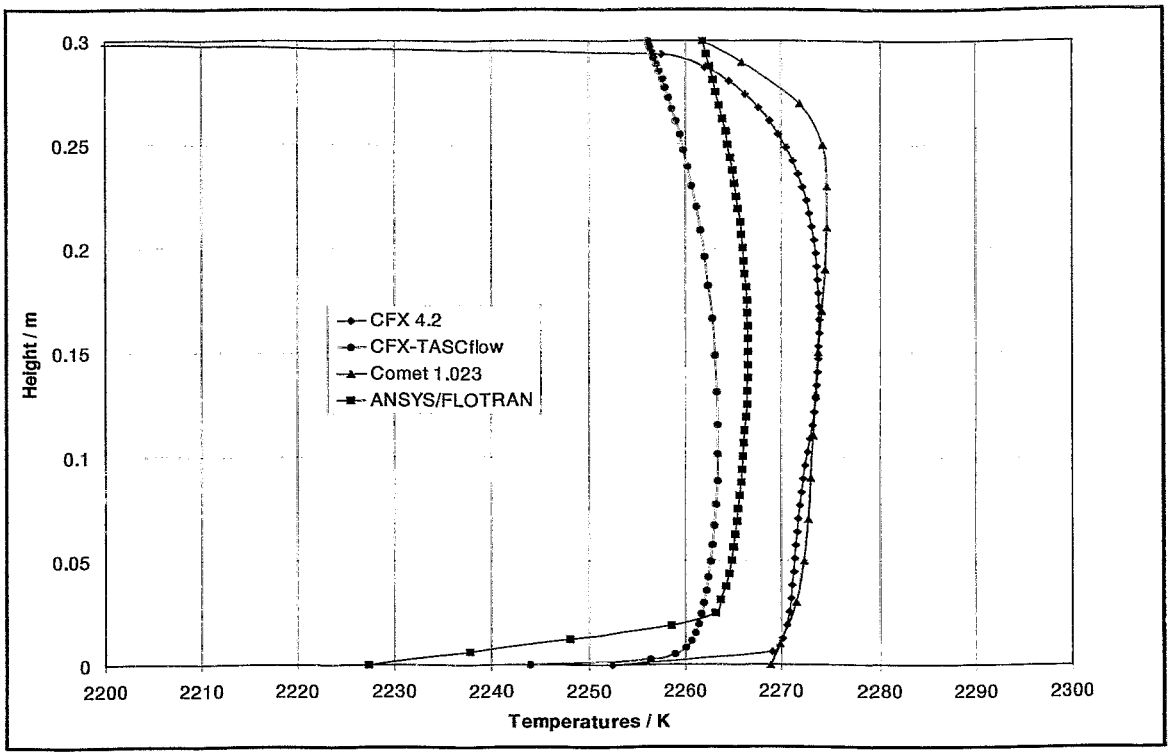

Fig. 11: Vertical temperature profiles of all codes at position X_3 after 2100 s.

5. Conclusion and Outlook

For the first stage of the benchmark calculations for an EPR-core catcher the 2D-ANSYS/FLOTRAN-calculations show a good agreement to the 3D-FVM-code calculations. This gives a basis for comparisons with the next calculations considering a separated melt of an oxidic layer and a metallic layer. These calculations have to be modeled with all codes as 2D-models because of limited computer resources.
With the assumed physical boundary conditions and material properties the selected numerical models do not predict a crust formation for the oxidic melt.
The behaviour of the melt temperature within the boundary layers has to be investigated and discussed more in detail, because it has not only consquences at the free surface of the melt pool but it affects also the fluid-fluid-boundary in the calculations to be performed in the future.

6. References

[1] Alsmeyer, H.; H. Werle: *Kernschmelzkühleinrichtungen für zukünftige DWR-Anlagen.* KfK-Nachrichten, Jahrg. 26, 3/1994, pp. 170-178.

[2] Steinwarz, W.; N. Dyllong; W. Koller: *COMAS Experiments for Representative Investigation on Core Melt Stabilization.* Proceedings of the TOPSAFE 98 Conference, Valencia, Spain, April 15-17, 1998.

[3] Fellmoser, F., G. Fieg, H. Massier, W. Schütz, U. Stegmaier, H. Werle: *Simulation Experiments on the Spreading Behaviour of Corium Melts.* Proceedings of the Jahrestagung Kerntechnik 1998, München 1998, ISSN 0720-9207.

[4] Göbel, A., M. Gonin, W. Korn: *Plant Layout. Video Presentation.* Proceedings of the European Pressurized Water Reactor Conference, Cologne 19.-21. October 1997.

[5] Allelein, H.-J., A. Breest, W. Erdmann, M. Heitsch, A. K. Rastogi, A. Scheuer, H.-G. Willschütz: Specification of the benchmark conditions, internal communications, meeting on the 14th of September 1998, internal report to be finished in 1999.

[6] Theofanous, T.G., C. Liu, S. Addition, S. Angelini, O. Kymäläinen, T. Salmassi: *In-vessel coolability and retention of a core melt.* Nucl. Eng. Des. 169, 1997, pp. 1-48.

[7] M. Schmidt, M. Wörner, G. Grötzbach: *Direkte numerische Simulation der Konvektion in einer Fluidschicht mit interner Wärmequelle.* FZKA 5916, 1997.

[8] Merker, G. P.: *Konvektive Wärmeübertragung.* Springer-Verlag, Berlin 1987.

[9] Launder, B.E., D.B. Spalding: *The Numerical Computation of Turbulent Flows.* Computer Methods in Applied Mechanics and Engineering 3, 1974, pp. 269-289.